

Copyright © 1973, by the author(s).  
All rights reserved.

Permission to make digital or hard copies of all or part of this work for personal or classroom use is granted without fee provided that copies are not made or distributed for profit or commercial advantage and that copies bear this notice and the full citation on the first page. To copy otherwise, to republish, to post on servers or to redistribute to lists, requires prior specific permission.

AN ALGORITHM FOR MODELING THE SINUSOIDAL INPUT/STEADY-  
STATE RESPONSE BEHAVIOR OF NONLINEAR SYSTEMS OVER  
A SET OF FREQUENCIES AND AMPLITUDES

by

L.O. Chua and R.J. Schilling

Memorandum No. ERL-M390

22 June 1973

ELECTRONICS RESEARCH LABORATORY

College of Engineering  
University of California, Berkeley  
94720

AN ALGORITHM FOR MODELING THE SINUSOIDAL INPUT/STEADY-  
STATE RESPONSE BEHAVIOR OF NONLINEAR SYSTEMS OVER  
A SET OF FREQUENCIES AND AMPLITUDES

by

L.O. Chua and R.J. Schilling

ABSTRACT

An algorithm for constructing a black box model of the sinusoidal input/steady-state response behavior of nonlinear time-invariant systems over a set of frequencies and amplitudes is presented. It is assumed that the steady-state response is periodic of the same fundamental frequency as the excitation, and that the Fourier coefficients are continuous functions of amplitude and square-integrable functions of frequency. The algorithm converges, in a mean-square sense, to an exact representation of the first  $N$  harmonics of the steady-state response minus its dc component. The model constructed by the algorithm admits a relatively simple physical realization characterized by  $2NM+1$  linear dynamic elements, and  $N(2M+1) + 1$  nonlinear static elements. The underlying mathematical structure of the model is an orthogonal series expansion relative to time whose coefficients are themselves truncated orthogonal expansions relative to frequency. Here  $M$ , the number of harmonics used for frequency interpolation, is determined by the algorithm. Of the  $N(2M+1) + 1$  memoryless nonlinearities which characterize the model,  $N$  of these are specified ahead of time (Tchebysheff polynomials), and  $2NM+1$  are parameters

---

Department of Electrical Engineering and Computer Sciences and the Electronics Research Laboratory, University of California, Berkeley, California, 94720.

Research sponsored in part by the U.S. Naval Electronic Systems Command, Contract N00039-71-C-0255, the National Science Foundation, Grant GK-32236, and Bell Telephone Laboratories, Doctoral Support Program, Case No. 78010-1.

which mold the representation to the specific system being modeled. Each of these functions of a single variable can be obtained in a pointwise manner directly from steady-state measurements. The algorithm was implemented on a digital computer, and forced versions of the classic equations of Van der Pol and Duffing were run as examples. An additional analytic example of a frequency multiplier of prescribed bandwidth was also presented.

## I. Introduction

The need for realistic yet tractable nonlinear device and system models has long been apparent. The current proliferation of nonlinear devices together with the growing emphasis on computer simulation point to the need for a modeling methodology which is not inherently dependent upon the internal mechanisms of the system or device being modeled. This invariably leads us to the black box or terminal perspective. Here the efforts of Volterra [14] and Wiener [15] have resulted in some very general nonlinear representation theorems. However practical problems are often encountered in identifying and representing the kernels required for these functional series representations. The  $N^{\text{th}}$  order kernel is a function of N variables. However no efficient computational algorithms are currently available for approximating surfaces of dimension greater than two. Hence until this computational bottleneck is overcome, the practical problems associated with the general modeling approach of Volterra and Wiener do not appear surmountable. Therefore it seems premature, if not unrealistic, to attempt to solve the general nonlinear modeling problem at this time. Indeed until we succeed in constructing models which can mimic the system response to a limited class of input signals, there is little hope that realistic practical models valid for more general classes of input signals will be discovered.

As a result we feel it is worthwhile to develop nonlinear representations valid for various classes of signals. The sinusoidal waveform in particular is an important paradigm signal around which to structure such a class. This signal finds extensive use in the electrical industry, especially with regard to electronic [6] and power systems [5]. We in-

tend to construct a model whose valid domain consists of sinusoidal signals whose frequencies and amplitudes range over any finite set of points in the open first quadrant of the frequency-amplitude plane.

Our fundamental assumption will be that the system response to such a signal tends to a steady-state waveform which is periodic of the same period as the excitation and expressible as a Fourier series. Hence we eliminate both subharmonics and incommensurate frequencies. More specifically we will assume that the Fourier coefficients of the steady-state response are:

- i) continuous functions of the amplitude of the excitation in a mean-square sense yet to be defined, and
- ii) square integrable (finite-energy) functions of the frequency of the excitation.

In addition we will place a uniform convergence requirement on the representation of the Fourier coefficients of the steady-state response with respect to frequency. This assumption will surface formally as a hypothesis of the convergence theorem of Algorithm 1.

Under these assumptions the algorithm we propose will converge in a mean-square sense to an exact representation of the first  $N$  harmonics of the steady-state response minus its dc (average) component. The model constructed by the algorithm will consist of an amplitude detection mechanism in tandem with a structure whose dynamics are segregated from the nonlinearity in a manner not unlike that done by Wiener [15]. As such the model admits a relatively simple physical realization characterized by  $2NM + 1$  dynamic elements. Here  $N$  and  $M$  denote the number of time and frequency harmonics used respectively.

The underlying mathematical structure of the model is an orthogonal series expansion relative to time whose coefficients are themselves truncated orthogonal expansions relative to frequency. The parameters which characterize the model are 2NM functions of a single variable. As a consequence the problem of identifying and representing these functions is relatively simple. Indeed, each of these functions can be obtained directly, in a pointwise manner, from steady-state terminal measurements.

The algorithm was implemented on a digital computer. As examples, forced versions of the classic equations of Van der Pol and Duffing were considered. In addition an analytic example of a frequency multiplier of prescribed bandwidth was presented. Finally the steady-state response characteristics of the amplitude detection subsystem were demonstrated.

Notationally we let  $\mathbb{R}_+$  denote the non-negative real numbers,  $\mathbb{N}$  the natural numbers,  $\mathcal{N}_k$  the set  $\{1, 2, \dots, k\}$ , and  $L^2(\mathbb{R}_+)$  the linear space of square-integrable functions defined on  $\mathbb{R}_+$ . Due to their frequent appearance, we denote the interval  $[1, \infty)$  by  $I$ , and the Cartesian products  $I \times I$  and  $\mathbb{R}_+ \times \mathbb{R}_+$  by  $I^2$  and  $\mathbb{R}_+^2$  respectively.

## II. Problem Formulation

Let  $S$  denote the nonlinear time-invariant system under consideration. We assume that  $S$  admits the standard 5-tuple dynamical system representation discussed in [4]:

$$(2.1) \quad \mathcal{R} \triangleq \{u, \Sigma, y, s, r\}$$

To conserve space we have adopted the notation defined in [4]. Here the input  $u: \mathbb{R}_+ \rightarrow \mathbb{R}$  and the output  $y: \mathbb{R}_+ \rightarrow \mathbb{R}$ . Let  $I \subset \mathbb{R}_+$  denote the

interval:

$$(2.2) \quad I \triangleq [1, \infty)$$

As the input set  $\mathcal{U}$  we take the following class of sinusoidal signals:

$$(2.3) \quad \mathcal{U} \triangleq \{u(t) = \lambda \cos(\omega t) \mid (t, \omega, \lambda) \in \mathbb{R}_+ \times I^2\}$$

Note that the lower bounds on the frequency  $\omega$  and the amplitude  $\lambda$  are not serious practical limitations since both may be scaled to suit the application (e.g. Hz, kHz, MHz). Consequently we are, in effect, considering frequencies and amplitudes anywhere in the open first quadrant of the frequency-amplitude plane.

Let the response function  $\rho: \mathbb{R}_+ \times \Sigma \times \mathcal{U} \rightarrow \mathbb{R}$  be defined in the standard manner:

$$(2.4) \quad \rho(t, x_0, u) \triangleq r(s(t, x_0, u), u(t))$$

We require that for each  $(x_0, u) \in \Sigma \times \mathcal{U}$  the system response  $\rho(\cdot, x_0, u)$  be ultimately periodic of the same fundamental frequency as the excitation  $u(\cdot)$ . More specifically we assume that the response to a sinusoidal input of frequency  $\omega$  and amplitude  $\lambda$  admits the following decomposition:

$$(2.5) \quad \rho(t, x_0, u) = \rho_T(t, x_0, u) + \rho_S(t, \omega, \lambda).$$

Here the transient component must satisfy:

$$(2.6) \quad \rho_T(t, x_0, u) \rightarrow 0 \text{ as } t \rightarrow \infty, \forall (x_0, u) \in \Sigma \times \mathcal{U},$$

and the steady-state component must be periodic of period  $2\pi/\omega$ :

$$(2.7) \quad \rho_S(t + \frac{2\pi}{\omega}, \omega, \lambda) = \rho_S(t, \omega, \lambda), \quad \forall (t, \omega, \lambda) \in \mathbb{R}_+ \times I^2$$

Furthermore we require that  $\rho_S(\cdot, \omega, \lambda)$  be expressible as a Fourier series [13]. Note that the steady-state response is, by hypothesis, independent of the initial condition,  $x_0 \in \Sigma$ .

We intend to model the transient behavior qualitatively and the steady-state behavior quantitatively. Let  $\mathcal{D} \subset \mathcal{U} \times \mathcal{Y}$  denote the set of input-output pairs (empirical data) upon which the model will be based.

$$(2.8) \quad \mathcal{D} \triangleq \mathcal{U} \times \{\rho_S(\cdot, \omega, \lambda) \mid (\omega, \lambda) \in I^2\}$$

We can then pose the modeling problem as follows.

Problem Statement:

Given  $\mathcal{D}$  construct a dynamical system  $\tilde{S}$  with response  $\tilde{\rho}(\cdot, \cdot, \cdot)$  such that for each  $(x_0, u) \in \Sigma \times \mathcal{U}$ :

$$(2.9) \quad \tilde{\rho}(t, \tilde{x}_0, u) = \tilde{\rho}_T(t, \tilde{x}_0, u) + \tilde{\rho}_S(t, \omega, \lambda), \quad \forall t \in \mathbb{R}_+$$

where:

$$(2.10) \quad \tilde{\rho}_T(t, \tilde{x}_0, u) \rightarrow 0 \text{ as } t \rightarrow \infty$$

and

$$(2.11) \quad \tilde{\rho}_S(t, \omega, \lambda) = \rho_S(t, \omega, \lambda), \quad \forall t \in \mathbb{R}_+$$

III. Preliminary Results

By hypothesis, the steady-state response admits a Fourier series representation. Let  $\rho_{SN}(\cdot, \omega, \lambda)$  denote the  $N^{\text{th}}$  partial sum of that series:

$$(3.1) \quad \rho_{SN}(t, \omega, \lambda) = \frac{a_0(\omega, \lambda)}{2} + \sum_{k=1}^N \{ a_k(\omega, \lambda) \cos(k\omega t) + b_k(\omega, \lambda) \sin(k\omega t) \}$$

Here

$$(3.2a) \quad a_k(\omega, \lambda) \triangleq \frac{\omega}{\pi} \int_0^{\frac{2\pi}{\omega}} \rho_S(t, \omega, \lambda) \cos(k\omega t) dt, \quad \forall k \in \mathbb{Z}_+$$

and

$$(3.2b) \quad b_k(\omega, \lambda) \triangleq \frac{\omega}{\pi} \int_0^{\frac{2\pi}{\omega}} \rho_S(t, \omega, \lambda) \sin(k\omega t) dt, \quad \forall k \in \mathcal{N}$$

We will restrict our consideration of the steady-state response to that component whose average value is zero. Hence we neglect the dc term of (3.1) by assuming:

$$(3.3) \quad a_0(\omega, \lambda) = 0, \quad \forall (\omega, \lambda) \in I^2$$

As we proceed, it will become apparent how to relax this assumption.

However we feel the added complexity it entails is not worthwhile since many systems do satisfy (3.3).

The algorithm we propose will converge in a mean-square sense to a model whose steady-state response is  $\rho_{SN}(\cdot, \omega, \lambda)$  where  $N \in \mathcal{N}$  is fixed but otherwise arbitrary.

#### A. Assumptions

Here we specify the requirements we place upon the Fourier coefficient functions  $a_k(\cdot, \cdot)$ , and  $b_k(\cdot, \cdot)$ ,  $\forall k \in \mathcal{N}_N$ . Ultimately we will restrict the

domain of the model to  $(\omega, \lambda) \in I^2$ . However we tactically assume that  $a_k(\cdot, \cdot)$  and  $b_k(\cdot, \cdot)$  are actually defined over  $\mathbb{R}_+^2$ .

### 1. Frequency Dependence

We assume that the Fourier coefficients of the steady-state response are square-integrable functions of frequency. More specifically for each

$$(\lambda, k) \in \mathbb{R}_+ \times \mathcal{N}_N:$$

$$(3.4a) \quad a_k(\cdot, \lambda) \in L^2(\mathbb{R}_+)$$

$$(3.4b) \quad b_k(\cdot, \lambda) \in L^2(\mathbb{R}_+)$$

Furthermore we will eventually require that an orthonormal series representation of these functions converge uniformly over  $\omega \in I$ . This requirement will surface formally as a hypothesis of the algorithm convergence theorem.

### 2. Amplitude Dependence

We assume that the Fourier coefficients are continuous functions of amplitude in the following mean-square sense. For each  $\epsilon > 0$ ,  $(\hat{\lambda}, k) \in \mathbb{R}_+ \times \mathcal{N}_N \exists \delta > 0 \ni |\lambda - \hat{\lambda}| < \delta \Rightarrow$

$$(3.5a) \quad \|a_k(\cdot, \lambda) - a_k(\cdot, \hat{\lambda})\|_{L^2} < \epsilon$$

and

$$(3.5b) \quad \|b_k(\cdot, \lambda) - b_k(\cdot, \hat{\lambda})\|_{L^2} < \epsilon$$

### B. Representation Relative to Frequency

Let  $\mathcal{L}_k$  denote the linear space of functions which are square-integrable

over the interval  $[\frac{1}{k}, \infty)$ :

$$(3.6) \quad \mathcal{L}_k \triangleq L^2([\frac{1}{k}, \infty))$$

The first result we need is concerned with the generation of an appropriate pair of complete orthonormal sets in  $\mathcal{L}_k$  which admits a simple yet direct system-theoretic interpretation and realization via circuit elements [12].

To that end consider the scalars:<sup>1</sup>

$$(3.7a) \quad \alpha_{k\ell} \triangleq \frac{(4k-1)^{1/2} \prod_{m=1}^{k-1} \{2(\ell+m)-1\}}{k \prod_{\substack{m=1 \\ m \neq \ell}} \{2(\ell-m)\}}, \quad \forall (k, \ell) \in \mathcal{N} \times \mathcal{N}_k$$

$$(3.7b) \quad \beta_{k\ell} \triangleq \frac{(4k+1)^{1/2} \prod_{m=1}^{k-1} \{2(\ell+m)+1\}}{k \prod_{\substack{m=1 \\ m \neq \ell}} \{2(\ell-m)\}}, \quad \forall (k, \ell) \in \mathcal{N} \times \mathcal{N}_k,$$

and the corresponding sets of functions they generate:

$$(3.8a) \quad \mathcal{A}_k \triangleq \{a_{k\ell}(\omega) \triangleq (k)^{1/2} \sum_{m=1}^{\ell} \frac{\alpha_{km}}{(k\omega)^{2m}} \mid (\omega, \ell) \in [\frac{1}{k}, \infty) \times \mathcal{N}\}$$

$$(3.8b) \quad \mathcal{B}_k \triangleq \{b_{k\ell}(\omega) \triangleq (k)^{1/2} \sum_{m=1}^{\ell} \frac{\beta_{km}}{(k\omega)^{2m-1}} \mid (\omega, \ell) \in [\frac{1}{k}, \infty) \times \mathcal{N}\}$$

### Proposition 1

For each  $k \in \mathcal{N}$ ,  $\mathcal{A}_k$  is a complete orthonormal set in  $\mathcal{L}_k$ . The

<sup>1</sup> Here for  $k = 1$  the factor  $\prod_{m=1}^0 \{2(\ell+m)+1\}$  is taken to be the multiplicative identity, 1.

same is true of  $\mathcal{B}_k$ .

Proof: We consider only the case of  $\mathcal{A}_k$ . The proof for  $\mathcal{B}_k$  does not differ in substance. Consider the set:

$$(3.9) \quad \mathcal{E} \triangleq \{e_\ell(\omega) \triangleq e^{-(2\ell - \frac{1}{2})\omega} \mid \forall \ell \in \mathcal{N}\}$$

and the linear map:

$$(3.10) \quad [U_k f](\omega) \triangleq (\omega)^{-1/2} f(\log(k\omega))$$

Now (3.9) and (3.10)  $\Rightarrow$

$$(3.11) \quad [U_k e_\ell](\omega) = \frac{(k)^{1/2}}{(k\omega)^{2\ell}}, \quad \forall (k, \ell) \in \mathcal{N}^2$$

Next (3.9) and (3.11)  $\Rightarrow$

$$(3.12) \quad \|e_\ell(\cdot)\|_{L^2} = \frac{1}{\sqrt{4\ell-1}} = \|[U_k e_\ell](\cdot)\|_{\mathcal{L}_k}$$

Hence  $U_k: \mathcal{E} \rightarrow \mathcal{L}_k$  is a unitary (norm-preserving) map, and the completeness properties of  $\mathcal{E}$  in  $L^2(\mathbb{R}_+)$  are identical to those of  $\{\frac{(k)^{1/2}}{(k\omega)^{2\ell}} \mid \forall \ell \in \mathcal{N}\}$  in  $\mathcal{L}_k$  [11].

From Clement [3],  $\mathcal{E}$  is complete in  $L^2(\mathbb{R}_+)$   $\Leftrightarrow$

$$(3.13) \quad \sum_{k=1}^N \frac{2k - \frac{1}{2}}{1 + (2k-1)^2} \rightarrow \infty \text{ as } N \rightarrow \infty$$

But  $\forall k > \frac{2}{3}$ :

$$(3.14) \quad \frac{2k - \frac{1}{2}}{1 + (2k-1)^2} > \frac{1}{2k}$$

Hence the series is bounded from below by a diverging (geometric) series, and the completeness of  $\{ \frac{\binom{k}{\ell}^{1/2}}{\binom{k\omega}{2\ell}} \mid \forall \ell \in \mathcal{N} \}$  in  $\mathcal{L}_k$  is established.

From Kautz [9], we can orthonormalize  $\mathcal{E}$  in  $L^2(\mathbb{R}_+)$  as:

$$(3.15) \quad e_\ell(\omega) \triangleq \sum_{m=1}^{\ell} \alpha_{\ell m} e_m(\omega), \quad \forall \ell \in \mathcal{N}$$

where  $\alpha_{\ell m}$  is as in (3.7a). Then (3.8a), (3.11), and the linearity of  $U_k \Rightarrow \mathcal{A}_k$  is a complete orthonormal set in  $\mathcal{L}_k$ .  $\square$

The sets  $\mathcal{A}_k$  and  $\mathcal{B}_k$  will appear in the model only in a limiting sense. Essentially we will employ linear subsystems  $H_{k\ell}(s)$  having the following property. As the poles of  $H_{k\ell}(s)$  approach the origin (and therefore instability), the real and imaginary components of the frequency response  $H_{k\ell}(j\omega)$  converge to  $a_{k\ell}(\omega)$  and  $b_{k\ell}(\omega)$  respectively. The objective of the following lemma is to establish the topology relative to which this convergence takes place. Let

$$(3.16a) \quad u_\ell(\omega, \mu) \triangleq \frac{1}{(\mu^2 + \omega^2)^\ell} \sum_{m=0}^{\lfloor \frac{\ell}{2} \rfloor} (-1)^m \binom{\ell}{2m} (\mu)^{\ell-2m} (\omega)^{2m}, \quad \forall (\omega, \mu) \in \mathbb{I} \times \mathbb{R}_+$$

$$(3.16b) \quad v_\ell(\omega, \mu) \triangleq \frac{1}{(\mu^2 + \omega^2)^\ell} \sum_{m=0}^{\lfloor \frac{\ell-1}{2} \rfloor} (-1)^m \binom{\ell}{2m+1} (\mu)^{\ell-2m-1} (\omega)^{2m+1}, \quad \forall (\omega, \mu) \in \mathbb{I} \times \mathbb{R}_+$$

and

$$(3.17) \quad \psi_\ell(\omega) \triangleq \frac{(-1)^{\lfloor \frac{\ell+1}{2} \rfloor}}{(\omega)^\ell}, \quad \forall \omega \in I$$

Here

$$(3.18) \quad \lfloor \frac{k}{2} \rfloor \triangleq \begin{cases} \frac{k}{2}, & k \text{ even} \\ \frac{k-1}{2}, & k \text{ odd} \end{cases}$$

and the binomial coefficient is defined:

$$(3.19) \quad \binom{\ell}{m} \triangleq \frac{\ell!}{m!(\ell-m)!}$$

Lemma 1

For each  $\ell \in \mathcal{N}$ :

$$(3.20a) \quad u_{2\ell}(\cdot, \mu) \xrightarrow{\mathcal{U}} \psi_{2\ell}(\cdot) \quad \text{as } \mu \rightarrow 0$$

$$(3.20b) \quad u_{2\ell-1}(\cdot, \mu) \xrightarrow{\mathcal{U}} \theta(\cdot) \quad \text{as } \mu \rightarrow 0$$

$$(3.21a) \quad v_{2\ell}(\cdot, \mu) \xrightarrow{\mathcal{U}} \theta(\cdot) \quad \text{as } \mu \rightarrow 0$$

$$(3.21b) \quad v_{2\ell-1}(\cdot, \mu) \xrightarrow{\mathcal{U}} \psi_{2\ell-1}(\cdot) \quad \text{as } \mu \rightarrow 0$$

where  $\theta(\cdot)$  denotes the zero function (identically zero on  $I$ ), and  $\mathcal{U}$  indicates convergence both uniformly over  $I$  and in the  $\mathcal{L}_1$  sense.

Proof: We consider only the case of  $u_\ell(\cdot, \cdot)$ . The dual argument for  $v_\ell(\cdot, \cdot)$  is nearly identical. From (3.16a):

$$(3.22) \quad |u_{2\ell-1}(\omega, \mu)| \leq \sum_{m=0}^{\ell-1} \binom{2\ell-1}{2m} (\mu)^{2(\ell-m)-1} (\omega)^{2(m-2\ell+1)}$$

Clearly (3.22)  $\Rightarrow$  (3.20b) both uniformly over I and in the  $\mathcal{L}_1$  norm.

Next (3.16a) and (3.17)  $\Rightarrow$

$$(3.23) \quad u_{2\ell}(\omega, \mu) - \psi_{2\ell}(\omega) = (-1)^\ell \left[ \left( \frac{\omega}{\mu^2 + \omega^2} \right)^{2\ell} - \left( \frac{1}{\omega} \right)^{2\ell} \right] \\ + \frac{1}{(\mu^2 + \omega^2)^{2\ell}} \sum_{m=0}^{\ell-1} (-1)^m \binom{2\ell}{2m} (\mu)^{2(\ell-m)} (\omega)^{2m}$$

Hence

$$(3.24) \quad |u_{2\ell}(\omega, \mu) - \psi_{2\ell}(\omega)| \leq \frac{(\mu^2 + \omega^2)^{2\ell} - (\omega)^{4\ell}}{(\omega)^{2\ell} (\mu^2 + \omega^2)^{2\ell}} \\ + \sum_{m=0}^{\ell-1} \binom{2\ell}{2m} (\mu)^{2(\ell-m)} (\omega)^{2(m-2\ell)}$$

A binomial expansion of the numerator of the first term then yields:

$$(3.25) \quad |u_{2\ell}(\omega, \mu) - \psi_{2\ell}(\omega)| \leq \sum_{m=0}^{2\ell-1} \binom{2\ell}{m} (\mu)^{2(2\ell-m)} (\omega)^{2(m-3\ell)} \\ + \sum_{m=0}^{\ell-1} \binom{2\ell}{2m} (\mu)^{2(\ell-m)} (\omega)^{2(m-2\ell)}$$

Finally (3.25)  $\Rightarrow$  (3.20a) both in the  $\mathcal{L}_1$  norm and uniformly over I.  $\square$

Note that  $u_\ell(\cdot, \mu)$  and  $v_\ell(\cdot, \mu)$  of (3.16) are nothing more than the real and imaginary components of the frequency response of a linear system with a pole at  $s = (-\mu, 0)$  of multiplicity  $\ell$  and unit residue.

C. Representation Relative to Amplitude

Consider the set of functions:

$$(3.26a) \quad \gamma_{k\ell}(\lambda) \triangleq \frac{1}{\pi} \int_{\frac{1}{k}}^{\infty} \int_0^{\frac{2\pi}{\omega}} \rho_S(t, \omega, \lambda) \cos(k\omega t) a_{k\ell}(\omega) \omega dt d\omega, \quad \forall (\lambda, k, \ell) \in \mathbb{R}_+ \times \mathcal{N} \times \mathcal{N}_k$$

$$(3.26b) \quad \delta_{k\ell}(\lambda) \triangleq \frac{1}{\pi} \int_{\frac{1}{k}}^{\infty} \int_0^{\frac{2\pi}{\omega}} \rho_S(t, \omega, \lambda) \sin(k\omega t) b_{k\ell}(\omega) \omega dt d\omega, \quad \forall (\lambda, k, \ell) \in \mathbb{R}_+ \times \mathcal{N} \times \mathcal{N}_k$$

Here  $a_{k\ell}(\cdot)$  and  $b_{k\ell}(\cdot)$  are as in (3.8).

Lemma 2

For each  $(k, \ell) \in \mathcal{N} \times \mathcal{N}_k$ , the functions  $\gamma_{k\ell}(\cdot)$  and  $\delta_{k\ell}(\cdot)$  are continuous.

Proof: From (3.2) and (3.26):

$$(3.27a) \quad \gamma_{k\ell}(\lambda) = \int_{\frac{1}{k}}^{\infty} a_k(\omega, \lambda) a_{k\ell}(\omega) d\omega$$

$$(3.27b) \quad \delta_{k\ell}(\lambda) = \int_{\frac{1}{k}}^{\infty} b_k(\omega, \lambda) b_{k\ell}(\omega) d\omega$$

Let  $(\lambda, \hat{\lambda}) \in \mathbb{R}_+^2$ . Then

$$(3.28) \quad \gamma_{k\ell}(\lambda) - \gamma_{k\ell}(\hat{\lambda}) = \int_{\frac{1}{k}}^{\infty} [a_k(\omega, \lambda) - a_k(\omega, \hat{\lambda})] a_{k\ell}(\omega) d\omega$$

Hence the Schwarz inequality  $\Rightarrow$

$$(3.29) \quad |\gamma_{k\ell}(\lambda) - \gamma_{k\ell}(\hat{\lambda})| \leq \|a_k(\cdot, \lambda) - a_k(\cdot, \hat{\lambda})\|_{C_k^0} \|a_{k\ell}(\cdot)\|_{C_k^0}$$

Then Proposition 1 (the normality of  $a_{k\ell}(\cdot)$ )  $\Rightarrow$

$$(3.30) \quad |\gamma_{k\ell}(\lambda) - \gamma_{k\ell}(\hat{\lambda})| \leq \|a_k(\cdot, \lambda) - a_k(\cdot, \hat{\lambda})\|_{C_k^0}$$

Finally the mean-square continuity of  $a_k(\cdot, \cdot)$  in (3.5)  $\Rightarrow \gamma_{k\ell}(\cdot)$  is continuous. A dual argument reveals that  $\delta_{k\ell}(\cdot)$  is also continuous.  $\square$

The functions  $\gamma_{k\ell}(\cdot)$  and  $\delta_{k\ell}(\cdot)$  are parameters which will appear in the model. Note from (2.8) that these parameters are determined solely on the basis of terminal information contained in the set of input-output pairs,  $\mathcal{D}$ .

Next consider the following first order nonlinear differential system:

$$(3.31) \quad \dot{x}(t) = f(u(t) - x(t)), \quad x(0) = x_0$$

Here  $f(\cdot)$  is a piecewise linear function defined as:

$$(3.32) \quad f(e) \triangleq \alpha e + \left[\frac{1}{\alpha} - \alpha\right] 1(e), \quad \forall e \in \mathbb{R}$$

where  $1(\cdot)$  denotes the unit step function:

$$(3.33) \quad 1(e) \triangleq \begin{cases} 1, & \forall e \geq 0 \\ 0, & \forall e < 0 \end{cases}$$

and

$$(3.34) \quad 0 < \alpha < 1$$

Lemma 3

For each  $(x_0, u) \in \mathbb{R} \times \mathcal{U}$  the system depicted in (3.31) has a unique solution  $x(\cdot, x_0, u)$ . Furthermore

$$(3.35) \quad x(t, x_0, u) \rightarrow x_g(t, \omega, \lambda) \text{ as } t \rightarrow \infty$$

where  $x_g(\cdot, \omega, \lambda)$  is continuous and periodic of period  $2\pi/\omega$ .

Proof: Refer to Appendix 1. □

Next we consider the effect of the scalar  $\alpha \in (0, 1)$  on the steady-state solution,  $x_g(\cdot, \omega, \lambda)$ .

Proposition 2

For each  $\epsilon > 0$ ,  $(x_0, u) \in \mathbb{R} \times \mathcal{U}$ ,  $\exists \delta > 0 \ni \alpha \in (0, \delta) \Rightarrow$

$$(3.36) \quad |x_g(t, \omega, \lambda) - \lambda| < \epsilon, \quad \forall t \in [0, \frac{2\pi}{\omega}]$$

Proof: Refer to Appendix 1. □

The function of the system depicted in (3.31) is to detect the amplitude  $\lambda$  of  $u(\cdot)$ . Any system whose steady-state response to  $u \in \mathcal{U}$  can be made to lie within an arbitrarily small band around  $\lambda \in I$  will

suffice. We offer (3.31) as one possible candidate for such an amplitude detection mechanism.

#### D. Representation of the Model

The model towards which we are working admits the following representation:

$$(3.37) \quad \dot{x}(t) = f(u(t) - x(t)), \quad x(0) = x_0$$

$$(3.38) \quad y_N(t) = \sum_{k=1}^N \int_0^t h_k(t-\tau, x(t)) \phi_k \left( \frac{u(\tau)}{x(\tau)} \right) d\tau$$

Here  $f(\cdot)$  is as in (3.32), and

$$(3.39) \quad \phi_k(z) \triangleq \begin{cases} T_k(-1), & \forall z \in (-\infty, -1) \\ T_k(z), & \forall z \in [-1, 1] \\ T_k(1), & \forall z \in (1, \infty) \end{cases}$$

where  $T_k(\cdot)$  denotes the  $k^{\text{th}}$  Tchebysheff polynomial of the  $1^{\text{st}}$  kind [1].

The impulse response surface  $h_k: \mathbb{R}_+ \times \mathbb{R}_+ \rightarrow \mathbb{R}$  is defined:

$$(3.40) \quad h_k(t, x) \triangleq (k)^{1/2} \sum_{\ell=1}^M \sum_{m=1}^{\ell} \left\{ (-1)^m \left[ \frac{\gamma_{k\ell}(x) \alpha_{\ell m} t^{2m-1}}{(2m)!} + \frac{\delta_{k\ell}(x) \beta_{\ell m} t^{2m-2}}{(2m-1)!} \right] e^{-\mu t} \right\}$$

where  $x$  denotes the output of the amplitude detector and where  $\gamma_{k\ell}(\cdot)$  and

$\delta_{k\lambda}(\cdot)$  are as in (3.26). The integer  $M \in \mathcal{N}$ , the scalar  $\mu > 0$ , and the scalar  $\alpha > 0$  (see (3.32)) are scalar parameters of the model which will be determined by the algorithm.

Lemma 4

For each  $\varepsilon > 0$ ,  $(k, u) \in \mathcal{N} \times \mathcal{U}$ ,  $\exists \delta > 0 \ni \alpha \in (0, \delta) \Rightarrow$

$$(3.41) \quad \phi_k \left( \frac{u(t)}{x_s(t, \omega, \lambda)} \right) = \text{Cos}(k\omega t) + e_{sk}(t, \omega, \lambda)$$

where

$$(3.42) \quad |e_{sk}(t, \omega, \lambda)| < \varepsilon, \quad \forall t \in \mathbb{R}_+$$

Here  $x_s(\cdot, \omega, \lambda)$  denotes the steady-state solution of (3.37).

Proof: From Proposition 2  $\exists \delta' > 0 \ni \alpha \in (0, \delta') \Rightarrow$

$$(3.43) \quad \left| \frac{u(t)}{x_s(t, \omega, \lambda)} - \text{Cos}(\omega t) \right| < \varepsilon, \quad \forall t \in [0, \frac{2\pi}{\omega}]$$

Then (3.39) and the uniform continuity of  $\phi_k(\cdot) \Rightarrow \exists \delta > 0 \ni \alpha \in (0, \delta) \Rightarrow$  (3.41) and (3.42).  $\square$

Lemma 5

For each  $\varepsilon > 0$ ,  $(k, \lambda) \in \mathcal{N} \times I$ ,  $\exists \delta > 0 \ni$

$$(3.44) \quad |e(t)| < \delta, \quad \forall t \in \mathbb{R}_+ \Rightarrow$$

$$(3.45) \quad \left| \int_0^t h_k(t-\tau, \lambda) e(\tau) d\tau \right| < \varepsilon, \quad \forall t \in \mathbb{R}_+$$

Proof: From (3.40) it suffices to consider the case:

$$(3.46) \quad \left| \int_0^t g_\lambda(t-\tau) e(\tau) d\tau \right| \leq \delta \int_0^t |g_\lambda(t-\tau)| d\tau$$

where

$$(3.47) \quad g_\lambda(t) \triangleq \frac{t^{\lambda-1} e^{-\mu t}}{\lambda!}, \quad \lambda \in \mathcal{N}$$

But

$$(3.48) \quad \int_0^t |g_\lambda(t-\tau)| d\tau \leq \|g_\lambda\|_{L^1}$$

where

$$(3.49) \quad \|g_\lambda\|_{L^1} \triangleq \int_0^\infty |g_\lambda(\tau)| d\tau = \frac{1}{\lambda(\mu)^\lambda} \quad \square$$

#### IV. The Algorithm

In order to devise an algorithm stop rule let  $\mathcal{T} \subset I \times I$  denote the set of "p" test frequencies and "q" test amplitudes relative to which we will measure the accuracy of the model.

$$(4.1) \quad \mathcal{T} \triangleq \{(\omega_i, \lambda_j) \in I^2 \mid \forall (i, j) \in \mathcal{N}_p \times \mathcal{N}_q\}$$

Relative to this set we then define a performance index:

$$(4.2) \quad \eta \triangleq \sum_{i=1}^p \sum_{j=1}^q \int_0^{\omega_i} [p_{SN}(t, \omega_i, \lambda_j) - y_{NS}(t, \omega_i, \lambda_j)]^2 dt$$

Here  $y_{NS}(\cdot, \omega, \lambda)$  denotes the steady-state response of the model to a sinusoidal input of frequency  $\omega$  and amplitude  $\lambda$ . Finally consider the functions

$$\hat{a}_{kj}: I \times \mathbb{R}_+ \rightarrow \mathbb{R} \text{ and } \hat{b}_{kj}: I \times \mathbb{R}_+ \rightarrow \mathbb{R}$$

defined:

$$(4.3a) \quad \hat{a}_{kj}(\omega, \mu) \triangleq (k)^{1/2} \sum_{\ell=1}^M \sum_{m=1}^{\ell} (-1)^m [\gamma_{k\ell}(\lambda_j) \alpha_{\ell m} u_{2m}(k\omega, \mu) + \delta_{k\ell}(\lambda_j) \beta_{\ell m} u_{2m-1}(k\omega, \mu)]$$

$$(4.3b) \quad \hat{b}_{kj}(\omega, \mu) \triangleq (k)^{1/2} \sum_{\ell=1}^M \sum_{m=1}^{\ell} (-1)^m [\gamma_{k\ell}(\lambda_j) \alpha_{\ell m} v_{2m}(k\omega, \mu) + \delta_{k\ell}(\lambda_j) \beta_{\ell m} v_{2m-1}(k\omega, \mu)]$$

where  $u_{\ell}(\cdot, \cdot)$  and  $v_{\ell}(\cdot, \cdot)$  are as in (3.16).

#### Algorithm 1

Step 0: Pick  $\epsilon > 0$ ,  $\mu > 0$ ,  $\alpha > 0$ ,  $k \in \mathcal{N}$ , and set  $\ell = 1$ . Typical values might be:

$$(4.4) \quad (\epsilon, \mu, \alpha, k) = (1, .5, .1, 10)$$

Step 1: Refer to (3.26). Compute  $\gamma_{k\ell}(\lambda_j)$  and  $\delta_{k\ell}(\lambda_j) \quad \forall (k, j) \in \mathcal{N}_N \times \mathcal{N}_q$ .

Step 2: Refer to (3.2) and (3.8) and (20). Compute

$$(4.5) \quad \epsilon_\ell \triangleq \sum_{i=1}^p \sum_{j=1}^q \sum_{k=1}^N \{ [a_k(\omega_i, \lambda_j) - \sum_{m=1}^{\ell} \gamma_{km}(\lambda_j) a_{km}(\omega_i)]^2 + [b_k(\omega_i, \lambda_j) - \sum_{m=1}^{\ell} \delta_{km}(\lambda_j) b_{km}(\omega_i)]^2 \}$$

Step 3: If  $\epsilon_\ell \geq \frac{\epsilon}{3}$ , set  $\ell = \ell + 1$  and go to step 1.

Step 4: Set  $M = \ell$  and refer to (4.3). Compute

$$(4.6) \quad \epsilon(\mu) \triangleq \sum_{i=1}^p \sum_{j=1}^q \sum_{k=1}^N \{ [a_k(\omega_i, \lambda_j) - \hat{a}_{kj}(\omega_i, \mu)]^2 + [b_k(\omega_i, \lambda_j) - \hat{b}_{kj}(\omega_i, \mu)]^2 \}$$

Step 5: If  $\epsilon(\mu) \geq \frac{2}{3} \epsilon$ , set  $\mu = \frac{\mu}{2}$  and go to step 4.

Step 6: Refer to (4.2) and compute the performance index  $\eta$ .

Step 7: If  $\eta \geq \epsilon$ , set  $\alpha = \frac{\alpha}{2}$  and go to step 6; otherwise, stop.

### Theorem 1

If the Fourier series representations of  $a_k(\cdot, \lambda)$  relative to  $\mathcal{A}_k$  and  $b_k(\cdot, \lambda)$  relative to  $\mathcal{B}_k$  converge uniformly over  $I, \forall (\lambda, k) \in I \times \mathcal{N}_N$ , then for each  $\epsilon > 0$  Algorithm 1 terminates in a finite number of iterations yielding a model with performance index  $\eta < \epsilon$ .

Proof: From (3.27),  $\gamma_{km}(\lambda)$  is the  $m^{\text{th}}$  Fourier coefficient of  $a_k(\cdot, \lambda)$  relative to the complete orthonormal set  $\mathcal{A}_k$ . Similarly  $\delta_{km}(\lambda)$  is the  $m^{\text{th}}$  Fourier coefficient of  $b_k(\cdot, \lambda)$  relative to  $\mathcal{B}_k$ . Hence (4.5) and the

uniform convergence hypothesis  $\Rightarrow \exists M \in \mathcal{N} \ni$

$$(4.7) \quad \epsilon_\ell < \frac{\epsilon}{3}, \quad \forall \ell \geq M$$

Next Lemma 1, (3.17), and (4.3)  $\Rightarrow$

$$(4.8a) \quad \hat{a}_{kj}(\cdot, \mu) \xrightarrow{\mathcal{L}} (k)^{1/2} \sum_{\ell=1}^M \sum_{m=1}^{\ell} \gamma_{k\ell}(\lambda_j) (-1)^m \alpha_{\ell m} \psi_{2m}(k \cdot) \quad \text{as } \mu \rightarrow 0$$

$$(4.8b) \quad \hat{b}_{kj}(\cdot, \mu) \xrightarrow{\mathcal{L}} (k)^{1/2} \sum_{\ell=1}^M \sum_{m=1}^{\ell} \delta_{k\ell}(\lambda_j) (-1)^m \beta_{\ell m} \psi_{2m-1}(k \cdot) \quad \text{as } \mu \rightarrow 0$$

where  $\mathcal{L}$  denotes uniform convergence over I.

Then (3.8) and (3.17)  $\Rightarrow$

$$(4.9a) \quad \hat{a}_{kj}(\cdot, \mu) \xrightarrow{\mathcal{L}} \sum_{\ell=1}^M \gamma_{k\ell}(\lambda_j) a_{k\ell}(\cdot) \quad \text{as } \mu \rightarrow 0$$

$$(4.9b) \quad \hat{b}_{kj}(\cdot, \mu) \xrightarrow{\mathcal{L}} \sum_{\ell=1}^M \delta_{k\ell}(\lambda_j) b_{k\ell}(\cdot) \quad \text{as } \mu \rightarrow 0$$

Hence (4.3), (4.5), and (4.6)  $\Rightarrow \exists \bar{\mu} > 0 \ni$

$$(4.10) \quad \epsilon(\mu) < \frac{2}{3} \epsilon, \quad \forall \mu \in (0, \bar{\mu})$$

Next refer to Lemma 4. Let  $y'_{NS}(\cdot, \omega, \lambda)$  and  $y''_{NS}(\cdot, \omega, \lambda)$  denote the steady-state solutions of (3.38) due to the sinusoidal and non-sinusoidal terms of (3.41) respectively.

Then (3.16), (3.40), and reference to a table of integrals [11]  $\Rightarrow$

$$\begin{aligned}
(4.11) \quad y'_{NS}(t, \omega, \lambda) = & \sum_{k=1}^N \sum_{\ell=1}^M \sum_{m=1}^{\ell} (k)^{1/2} (-1)^m \{ [\gamma_{k\ell}(x_s(t, \omega, \lambda)) \alpha_{\ell m} u_{2m}(k\omega, \mu) \\
& + \delta_{k\ell}(x_s(t, \omega, \lambda)) \beta_{\ell m} u_{2m-1}(k\omega, \mu)] \cos(k\omega t) + [\gamma_{k\ell}(x_s(t, \omega, \lambda)) \alpha_{\ell m} v_{2m}(k\omega, \mu) \\
& + \delta_{k\ell}(x_s(t, \omega, \lambda)) \beta_{\ell m} v_{2m-1}(k\omega, \mu)] \sin(k\omega t) \}
\end{aligned}$$

Next (4.3), Proposition 1, and the continuity of  $\gamma_{k\ell}(\cdot)$  and  $\delta_{k\ell}(\cdot) \Rightarrow \exists \alpha' > 0 \ni \alpha \in (0, \alpha') \Rightarrow$

$$\begin{aligned}
(4.12) \quad \sum_{i=1}^p \sum_{j=1}^q \int_0^{\frac{2\pi}{\omega_i}} \{ y'_{NS}(t, \omega_i, \lambda_j) - \sum_{k=1}^N [\hat{a}_{kj}(\omega_i, \mu) \cos(k\omega_i t) \\
+ \hat{b}_{kj}(\omega_i, \mu) \sin(k\omega_i t)] \}^2 dt < \frac{\epsilon}{6}
\end{aligned}$$

Hence (4.6) and (4.10)  $\Rightarrow \exists \alpha'' \in (0, \alpha') \ni \alpha \in (0, \alpha'') \Rightarrow$

$$(4.13) \quad \sum_{i=1}^p \sum_{j=1}^q \int_0^{\frac{2\pi}{\omega_i}} [\rho_{SN}(t, \omega_i, \lambda_j) - y'_{NS}(t, \omega_i, \lambda_j)]^2 dt < \frac{5}{6} \epsilon$$

Finally consider  $y''_{NS}(\cdot, \omega, \lambda)$ , the steady-state response (3.38) due to the non-sinusoidal term of (3.41). From Lemma 4, (3.40), Lemma 5, and the continuity of  $h_k(t, \cdot) \exists \bar{\alpha} \in (0, \alpha'') \ni \alpha \in (0, \bar{\alpha}) \Rightarrow$

$$(4.14) \quad \sum_{i=1}^p \sum_{j=1}^q \int_0^{\frac{2\pi}{\omega_i}} [y''_{SN}(t, \omega_i, \lambda_j)]^2 dt < \frac{\epsilon}{6}$$

Then (4.2), (4.13), and the triangle inequality  $\Rightarrow \eta < \epsilon. \quad \square$

## 2. Physical Realization

Our objective here is to obtain a physical realization of the model depicted in (3.37) and (3.38) which is minimal in the sense that exactly  $2NM + 1$  dynamic elements are required. We will employ ideal elements. Hence we neglect loading effects in this realization. Consider the set of functions:

$$(4.15a) \quad \boxed{\epsilon_{k,2m}(\lambda) \triangleq (-1)^m (k)^{1/2} \sum_{\ell=m}^M \alpha_{\ell m} \gamma_{k\ell}(\lambda)}, \quad \forall (k,m,\lambda) \in \mathcal{N}_N \times \mathcal{N}_M \times \mathbb{R}_+$$

$$(4.15b) \quad \boxed{\epsilon_{k,2m-1}(\lambda) \triangleq (-1)^m (k)^{1/2} \sum_{\ell=m}^M \beta_{\ell m} \delta_{k\ell}(\lambda)}, \quad \forall (k,m,\lambda) \in \mathcal{N}_N \times \mathcal{N}_M \times \mathbb{R}_+$$

### Proposition 3

The model depicted in (3.37) and (3.38) can be realized with the system shown in Fig. 1 and Fig. 2. This realization is minimal.

Proof: Refer to Fig. 1. The output of the integrator is constrained to satisfy:

$$(4.16) \quad \dot{x}(t) = f(u(t) - x(t)), \quad x(0) = x_0$$

Hence this realizes the amplitude detection subsystem of (3.37). The memoryless subsystems  $\phi_k(\cdot)$ ,  $\forall k \in \mathcal{N}$  can then be realized with nonlinear resistors [2].

It remains to realize the impulse response surface  $h_k(\cdot, \cdot)$ . Refer to Fig. 2. Here the response to an impulse is modulated by  $x(\cdot)$ , the

output of the amplitude detection system, as follows:

$$(4.17) \quad \hat{h}_k(t, x) = \sum_{\ell=1}^{2M} \xi_{k\ell}(x) \frac{t^{\ell-1} e^{-\mu t}}{\ell!}$$

Hence (4.15)  $\Rightarrow$

$$(4.18) \quad \hat{h}_k(t, x) = (k)^{1/2} \sum_{\ell=1}^M \sum_{m=\ell}^M (-1)^\ell \left[ \frac{\gamma_{k\ell}(x) \alpha_{m\ell} t^{2\ell-1}}{(2\ell)!} + \frac{\delta_{k\ell}(x) \beta_{m\ell} t^{2\ell-2}}{(2\ell-1)!} \right] e^{-\mu t}$$

Re-ordering the summation then yields:

$$(4.19) \quad \hat{h}_k(t, x) = (k)^{1/2} \sum_{\ell=1}^M \sum_{m=1}^{\ell} (-1)^m \left[ \frac{\gamma_{k\ell}(x) \alpha_{\ell m} t^{2m-1}}{(2m)!} + \frac{\delta_{k\ell}(x) \beta_{\ell m} t^{2m-2}}{(2m-1)!} \right] e^{-\mu t}$$

Finally (3.40)  $\Rightarrow$

$$(4.20) \quad \hat{h}_k(t, x) = h_k(t, x), \quad \forall (t, x) \in \mathbb{R}_+^2 \quad \square$$

Note from Fig. 2 that the transfer function  $1/(s+\mu)$  can be readily realized with a linear capacitor, two linear resistors, and an operational amplifier [8].

## V. Applications

In order to substantiate the theoretic claims made thus far, we consider a number of examples.

### 1. The Forced Van der Pol Equation

Consider the following second order nonlinear differential system due

to Van der Pol [7]:

$$(5.1) \quad \ddot{y} + y(1-y^2)\dot{y} = u(t)$$

In this example the scalar parameters of the model were chosen as follows:

$$(5.2) \quad (\alpha, \mu, M) = \left( \frac{1}{10\pi}, \frac{1}{10}, 2 \right)$$

Here  $\alpha$  characterizes the function  $f(\cdot)$  of (3.32),  $\mu$  denotes the location of the poles of the impulse response surface  $h_k(\cdot, \cdot)$  of (3.40), and  $M$  is the number of harmonics used for interpolation relative to frequency.

In order to graphically demonstrate the convergence rate with respect to the number of time harmonics,  $N$ , two cases were considered. In Fig. 3 we display the results for  $N = 3$  harmonics. Two frequencies and two amplitudes were plotted. The solid line indicates the response of the system, and the dashed line the response of the model. In Fig. 4 the same results are plotted for  $N = 6$  harmonics. Notice that the terminal behavior of the model undergoes a definite improvement. However even with as few as  $N = 3$  harmonics the "fit" to the empirical data (area between solid and dashed curves) is encouraging.

## 2. The Forced Duffing Equation

Consider the following second order nonlinear differential system due to Duffing [7]:

$$(5.3) \quad \ddot{y} + y[1+y^2] + \dot{y} = u(t)$$

Duffing's equation is, of course, known to exhibit subharmonic solutions under certain conditions. Care was taken to see that these conditions

were not satisfied since this would clearly violate one of our assumptions. In this example the scalar parameters of the model were chosen as follows:

$$(5.4) \quad (\alpha, \mu, M) = \left( \frac{1}{10\pi}, \frac{1}{10}, 2 \right)$$

The results of the model are displayed in Fig. 5 for  $N = 6$  harmonics. Again the performance of the model is accurate qualitatively, and (for the number of harmonics employed) a good fit quantitatively.

### 3. A Frequency Multiplier of Prescribed Bandwidth

Here we consider an analytic example. We model a nonlinear system which multiplies the frequency of the excitation by a factor of  $n \in \mathcal{N}$  over the interval  $\omega \in [1, \bar{\omega}]$ . Hence

$$(5.5) \quad \rho_S(t, u) = \begin{cases} \lambda \cos(n\omega t), & \forall (t, \omega, \lambda) \in \mathbb{R}_+ \times [1, \bar{\omega}] \times I \\ 0, & \forall (t, \omega, \lambda) \in \mathbb{R}_+ \times (\bar{\omega}, \infty) \times I \end{cases}$$

Refer to (3.8) and (3.27). Here

$$(5.6) \quad \gamma_{n\ell}(\lambda) = \lambda(n)^{1/2} \sum_{k=1}^{\ell} \frac{\alpha_{nk}}{1-2k} [(n\bar{\omega})^{1-2k} - 1]$$

Following simplification the model can then be stated as:

$$(5.7) \quad \dot{x}(t) = f(u(t) - x(t)), \quad x(0) = x_0$$

$$(5.8) \quad y(t) = x(t) \int_0^t g_n(t-\tau) \phi_n \left( \frac{u(\tau)}{x(\tau)} \right) d\tau$$

where:

$$(5.9) \quad g_n(t) \stackrel{\Delta}{=} n \sum_{\ell=1}^M \sum_{m=1}^{\ell} \sum_{k=1}^{\ell} \frac{(-1)^m \alpha_{nk}^{\alpha} \ell_m [(n\omega)^{1-2k} - 1]}{(1-2k)} \frac{t^{2m-1} e^{-\mu t}}{(2m)!}$$

#### 4. An Amplitude Detection Example

Here we graphically display the steady-state response behavior of the amplitude detection subsystem depicted in (3.31). The results are shown in Fig. 6 where we plotted the steady-state response  $x_g(\cdot, \omega, \lambda)$  against the input  $u(\cdot)$  for two values of frequency and two values of amplitude. In this example the scalar parameter chosen was as follows:

$$(5.10) \quad \alpha = \frac{1}{10\pi}$$

Note that the peak-to-peak "ripple" in the steady-state response  $x_g(\cdot, \omega, \lambda)$  is larger for lower frequencies as one would expect. However in all cases the normalized error is of the order of two percent. We know from Proposition 2 that this result can be reduced by decreasing  $\alpha$ , but only at the expense of more sluggish transient behavior (try  $x_0 > \lambda$ ).

#### VI. Conclusions

We have proposed an algorithm which converges to a model whose valid domain consists of sinusoidal signals with frequencies and amplitudes ranging over any finite set of points in the open first quadrant of the frequency-amplitude plane.

The principal assumptions placed upon the nonlinear time-invariant system being modeled were the following:

- 1) The response to a sinusoidal input tends to a steady-state waveform which is periodic of the same period as the excitation and expressible as a

Fourier series.

ii) The Fourier coefficients of the steady-state response are continuous functions of amplitude in the mean-square sense indicated in (3.5).

iii) The Fourier coefficients of the steady-state response are square-integrable functions of frequency. More specifically the convergence of their representations relative to the complete orthonormal sets of (3.8) must be uniform over  $\omega \in I$ .

It was shown that under these assumptions the algorithm converges in a mean-square sense to an exact representation of the first  $N$  harmonics of the steady-state response minus its dc (average) component. Here the natural number  $N$  is fixed during initialization of the algorithm, but is otherwise arbitrary.

The model constructed by the algorithm consists of an amplitude detection mechanism in tandem with a structure whose dynamics are segregated from the nonlinearity in a manner similar to that done by Wiener [15]. As such the model admits a relatively simple physical realization characterized by  $2NM + 1$  linear dynamic elements, and  $N(2M+1) + 1$  nonlinear static elements. Here the natural number  $M$  denotes the number of terms (harmonics) used for interpolation relative to frequency. It is determined by the algorithm. The underlying mathematical structure of the model is an orthogonal series expansion relative to time whose coefficients are themselves truncated orthogonal series expansions relative to frequency. The basis functions used for frequency interpolation are nothing more than the frequency responses of simple linear subsystems. It was shown that as the poles of these linear

subsystems tend to the origin, the frequency responses tend (both uniformly and in a mean-square sense) to a set of functions  $A_k$  and  $B_k$  which were shown to be complete and orthonormal in  $L_k$ .

Of the  $N(2M+1) + 1$  memoryless nonlinearities employed in the realization,  $N$  of these are specified ahead of time (the Tchebysheff polynomials), and the remaining  $2NM + 1$  are parameters used to "mold" the representation to the specific system being modeled. Each of the characterizing functions can be obtained in a pointwise fashion directly from steady-state measurements of the system. They are, in fact, nothing more than the generalized Fourier coefficients (relative to frequency) of the classic Fourier coefficients (relative to time) of the steady-state response. As such they are functions of a single variable, the amplitude of the excitation. It was pointed out that any amplitude detection subsystem having the properties of the (first order) one we cited would suffice.

Finally we acknowledge that a shortcoming of the model we have proposed is the necessary trade off between accuracy and speed. As the desired accuracy increases, the transient behavior of the model becomes more sluggish. However it was pointed out in the problem formulation that our intention was to model the transient behavior qualitatively, and the steady-state behavior quantitatively. The algorithm was implemented on a digital computer, and several examples were run. We considered forced versions of the classic equations of Van der Pol and Duffing. In both cases the results substantiated the theoretic claims we have put forward. An analytic example of a frequency multiplier of prescribed bandwidth was also presented. Finally the steady-state response characteristics of the amplitude detection subsystem were demonstrated graphically. The necessary

stability around the amplitude of the excitation was confirmed for several frequencies and amplitudes.

## Appendix 1

### A. Proof of Lemma 3

Refer to (2.3) and (3.32). Let

$$(A.1) \quad g(x(t), t) \stackrel{\Delta}{=} f(u(t) - x(t))$$

Then (3.31) can be stated

$$(A.2) \quad \dot{x} = g(x, t), \quad x(0) = x_0$$

From (3.34)  $g(\cdot, t)$  is Lipschitzian with Lipschitz constant  $\frac{1}{\alpha} > 0$  [7].

Hence  $\exists$  a unique  $x: \mathbb{R}_+ \times \mathbb{R} \rightarrow \mathbb{R} \ni$

$$(A.3) \quad \dot{x}(t, x_0) = g(x(t, x_0), t), \quad \forall (t, x_0) \in \mathbb{R}_+ \times \mathbb{R}$$

and

$$(A.4) \quad x(0, x_0) = x_0, \quad \forall x_0 \in \mathbb{R}.$$

Suppose

$$(A.5) \quad x(t, x_0) \rightarrow \underline{+\infty} \text{ as } t \rightarrow \infty$$

It follows from (3.32) that

$$(A.6) \quad \dot{x}(t, x_0) \rightarrow \bar{+\infty} \text{ as } t \rightarrow 0$$

But this is a contradiction. Hence for each  $x_0 \in \mathbb{R} \exists M > 0 \ni$

$$(A.7) \quad |x(t, x_0)| \leq M, \quad \forall t \in \mathbb{R}_+$$

Then from Massera [10]  $\exists x_s: \mathbb{R}_+ \rightarrow \mathbb{R} \ni$

$$(A.8) \quad \dot{x}_s(t) = g(x_s(t), t), \quad \forall t \in \mathbb{R}_+$$

and

$$(A.9) \quad x_s(t + \frac{2\pi}{\omega}) = x_s(t), \quad \forall t \in \mathbb{R}_+$$

where  $\omega \in [1, \infty)$  is the frequency of  $u(\cdot)$ .

Next we will show that for each  $x_0 \in \mathbb{R}$ , the unique solution  $x(\cdot, x_0)$  is asymptotic to the periodic solution  $x_s(\cdot)$ .

Let  $(t_0, x_0) \in \mathbb{R}_+ \times \mathbb{R}$ . We consider three cases.

Suppose  $x(t_0, x_0) > x_s(t_0)$ . Then (3.32) and (3.33)  $\Rightarrow \dot{x}(t_0, x_0) < \dot{x}_s(t_0)$ .

Suppose  $x(t_0, x_0) = x_s(t_0)$ . Then the uniqueness of  $x(\cdot, \cdot) \Rightarrow x(t, x_0) = x_s(t)$ ,  $\forall t \in [t_0, \infty)$ .

Finally suppose  $x(t_0, x_0) < x_s(t_0)$ . In this case (3.32) and (3.33)  $\Rightarrow \dot{x}(t_0, x_0) > \dot{x}_s(t_0)$ . It follows that for each  $x_0 \in \mathbb{R}$ :

$$(A.10) \quad |x(t, x_0) - x_s(t)| \rightarrow 0 \text{ as } t \rightarrow \infty$$

## B. Proof of Proposition 2

Here we let the dependence of the steady-state solution on  $\omega$  and  $\lambda$  surface formally as additional arguments. Suppose

$$(A.11) \quad x_s(t_0, \omega, \lambda) \geq \lambda + \varepsilon, \text{ for some } t_0 \in \mathbb{R}$$

Let

$$(A.12) \quad \delta_0 \triangleq \min \left\{ 1, \frac{\omega \varepsilon}{2\pi(2\lambda + \varepsilon)} \right\}$$

Then (3.32), (3.33) and  $\alpha \in (0, \delta_0) \Rightarrow$

$$(A.13) \quad \dot{x}_s(t_0 + T, \omega, \lambda) < 0, \quad \forall T \in [0, \frac{2\pi}{\omega}]$$

But this contradicts the periodicity of  $x_s(\cdot, \omega, \lambda)$ . Hence  $\alpha \in (0, \delta_0) \Rightarrow$

$$(A.14) \quad x_s(t, \omega, \lambda) < \lambda + \varepsilon, \quad \forall t \in [0, \frac{2\pi}{\omega}]$$

Let  $\Delta x_s(\omega, \lambda)$  denote the peak-to-peak ripple of  $x_s(\cdot, \omega, \lambda)$ .

$$(A.15) \quad \Delta x_s(\omega, \lambda) \triangleq \max_{t \in [0, \frac{2\pi}{\omega}]} x_s(t, \omega, \lambda) - \min_{t \in [0, \frac{2\pi}{\omega}]} x_s(t, \omega, \lambda)$$

Then (3.32), (3.33), and  $\alpha \in (0, \delta_0) \Rightarrow$

$$(A.16) \quad \Delta x_s(\omega, \lambda) < \varepsilon$$

Suppose

$$(A.17) \quad x_s(t, u) \leq \lambda - \varepsilon, \quad \forall t \in [0, \frac{2\pi}{\omega}]$$

Then  $\exists (t_1, \delta_1) \in (0, \frac{2\pi}{\omega}] \times (0, t_1]$  independent of  $\alpha \Rightarrow$

$$(A.18) \quad u(t) - x_s(t, u) > \frac{\varepsilon}{2}, \quad \forall t \in [t_1 - \delta_1, t_1 + \delta_1]$$

Hence (3.32), (3.33) and (A.15)  $\Rightarrow$

$$(A.19) \quad \Delta x_s(\omega, \lambda) > \frac{\varepsilon \delta_1}{\alpha}$$

Let

$$(A.20) \quad \delta_2 \triangleq \min\{\delta_0, \delta_1\}$$

Then  $\alpha \in (0, \delta_2)$  and (A.19)  $\Rightarrow$  a contradiction of (A.16). Hence

$$\alpha \in (0, \delta_2) \Rightarrow$$

$$(A.21) \quad |x_s(t_0, u) - \lambda| < \varepsilon, \text{ for some } t_0 \in [0, \frac{2\pi}{\omega}]$$

Finally (A.21) and a re-application of the fact that

$$(A.22) \quad \Delta x_s(\omega, \lambda) \rightarrow 0 \text{ as } \alpha \rightarrow 0$$

$$\Rightarrow \exists \delta \in (0, \delta_2) \ni \alpha \in (0, \delta) \Rightarrow$$

$$(A.23) \quad |x_s(t, \omega, \lambda) - \lambda| < \varepsilon, \quad \forall t \in [0, \frac{2\pi}{\omega}]$$

□

### List of References

1. M. Abramowitz and I.A. Stegun, Handbook of Mathematical Functions, Dover, New York, 1965.
2. L.O. Chua, Introduction to Nonlinear Network Theory, McGraw-Hill, New York, 1969.
3. P.R. Clement, "On Completeness of Basis Functions Used for Signal Analysis," SIAM Review, 5(1963), pp. 131-139.
4. C.A. Desoer, Notes for a Second Course on Linear Systems, Van Nostrand Reinhold, New York, 1970.
5. O.E. Elgerd, Electric Energy Systems Theory: An Introduction, McGraw-Hill, New York, 1971.
6. P.E. Gray and C.L. Searle, Electronic Principles: Physics, Models, and Circuits, Wiley, New York, 1969.
7. J.K. Hale, Ordinary Differential Equations, Wiley, New York, 1969.
8. A.S. Jackson, Analog Computation, McGraw-Hill, New York, 1960.
9. W.H. Kautz, "Transient Synthesis in the Time Domain," IRE Trans. Circuit Theory, CT-1(1954), pp. 29-39.
10. J.L. Massera, "The Existence of Periodic Solutions of Systems of Differential Equations," Duke Math. J., 17(1950), pp. 457-475.
11. R. Paley and N. Wiener, Fourier Transforms in the Complex Domain, Am. Math. Soc. Colloquium Pub., Providence, R.I., Vol. XIX, 1934.
12. G. Szego, Orthonormal Polynomials, American Math. Society, Rhode Island, Vol. XXIII, 3rd. ed., 1967.
13. G.P. Tolstov, Fourier Series, Prentice-Hall, Englewood Cliff, N.J., 1962.

14. V. Volterra, Theory of Functionals and of Integral and Integro-Differential Equations, Dover Publications, New York, 1959.
15. N. Wiener, Nonlinear Problems in Random Theory, Wiley, New York, 1958.

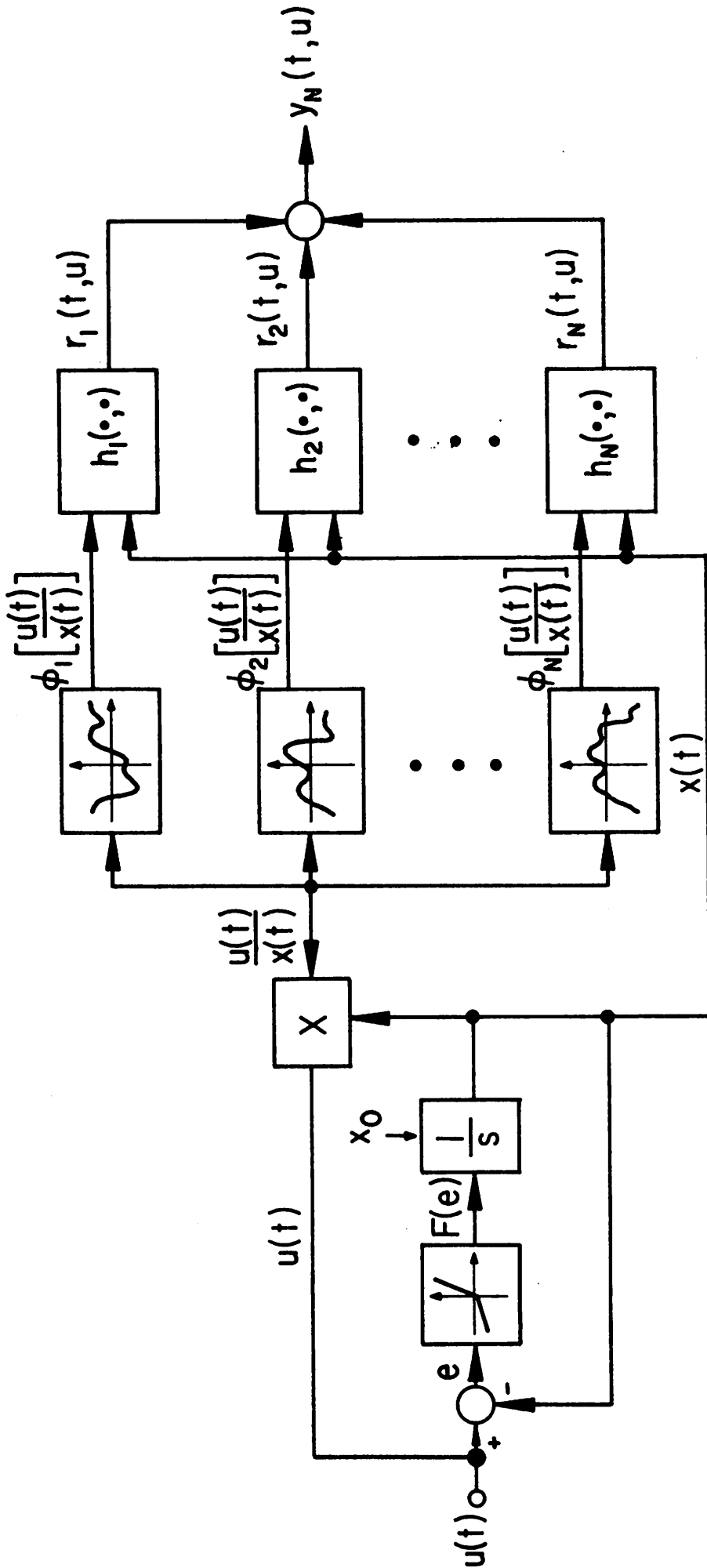


Fig. 1. Realization of Sinusoidal Input-Steady-State Response Model.

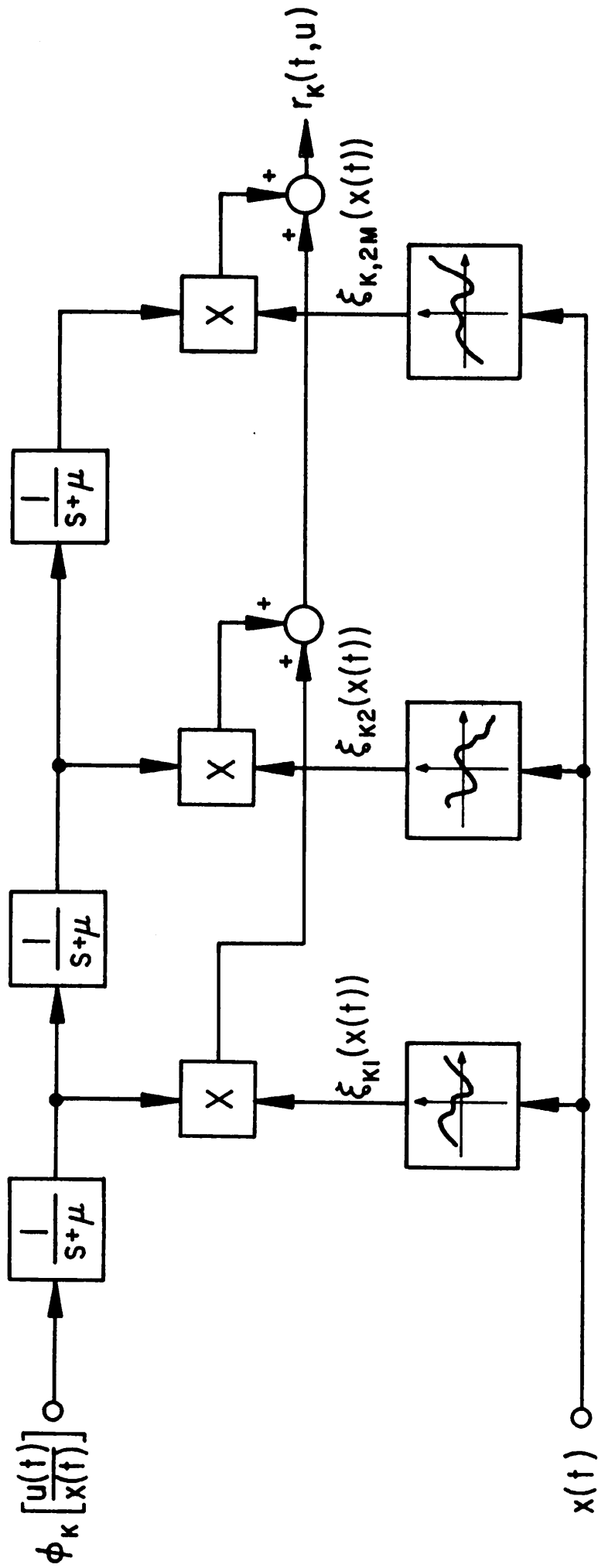


Fig. 2. Realization of Linear Subsystem Characterized by the Impulse Response Surface  $h_k(\cdot, \cdot, \cdot)$ .

FREQUENCY

$\triangle$  = 1

$\nabla$  = 2

PLOT KEY

— = DATA

- - - = MODEL

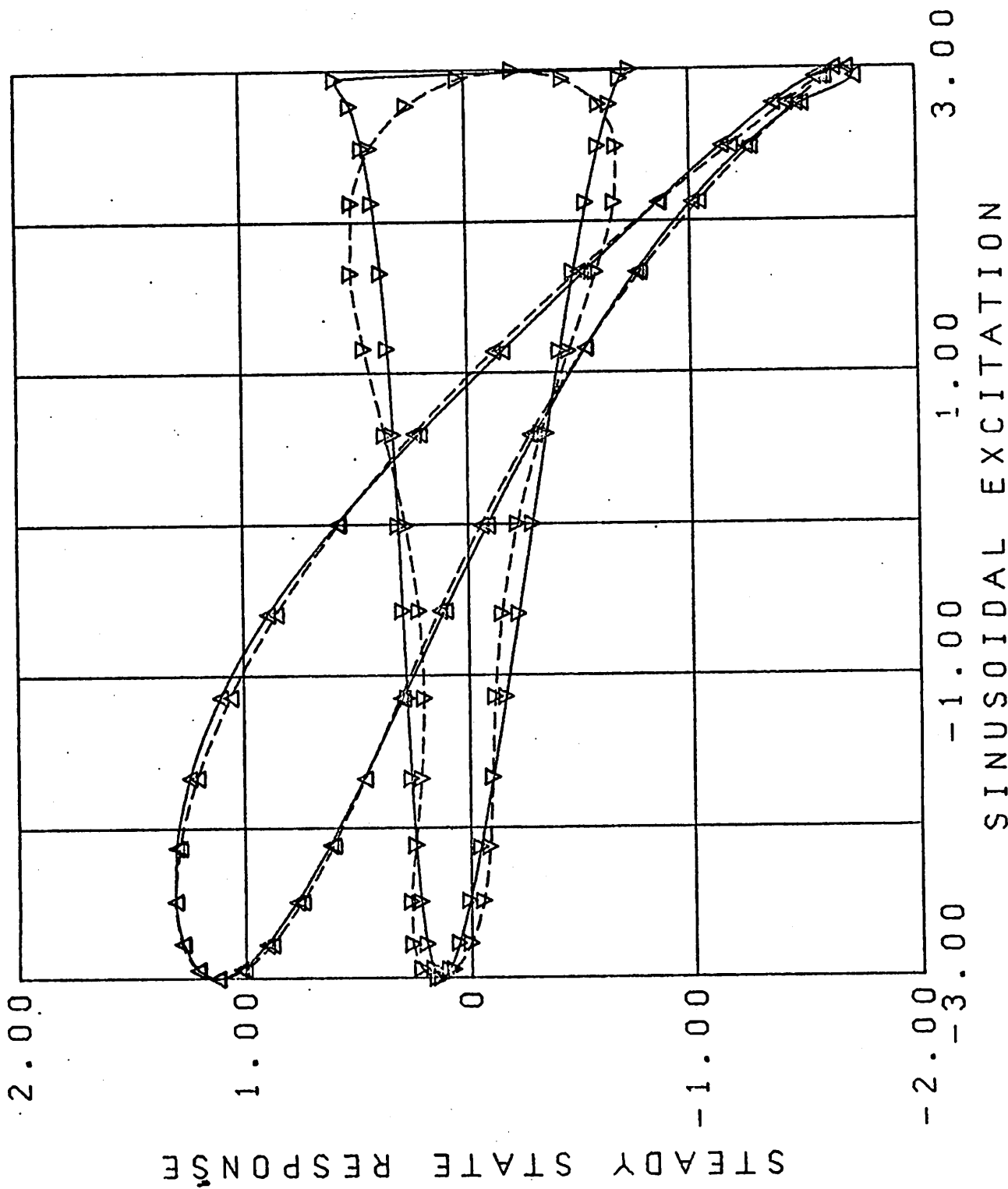


Fig. 3a. Steady State Response of System and Model for the Forced Van der Pol Equation with  $N = 3$ .

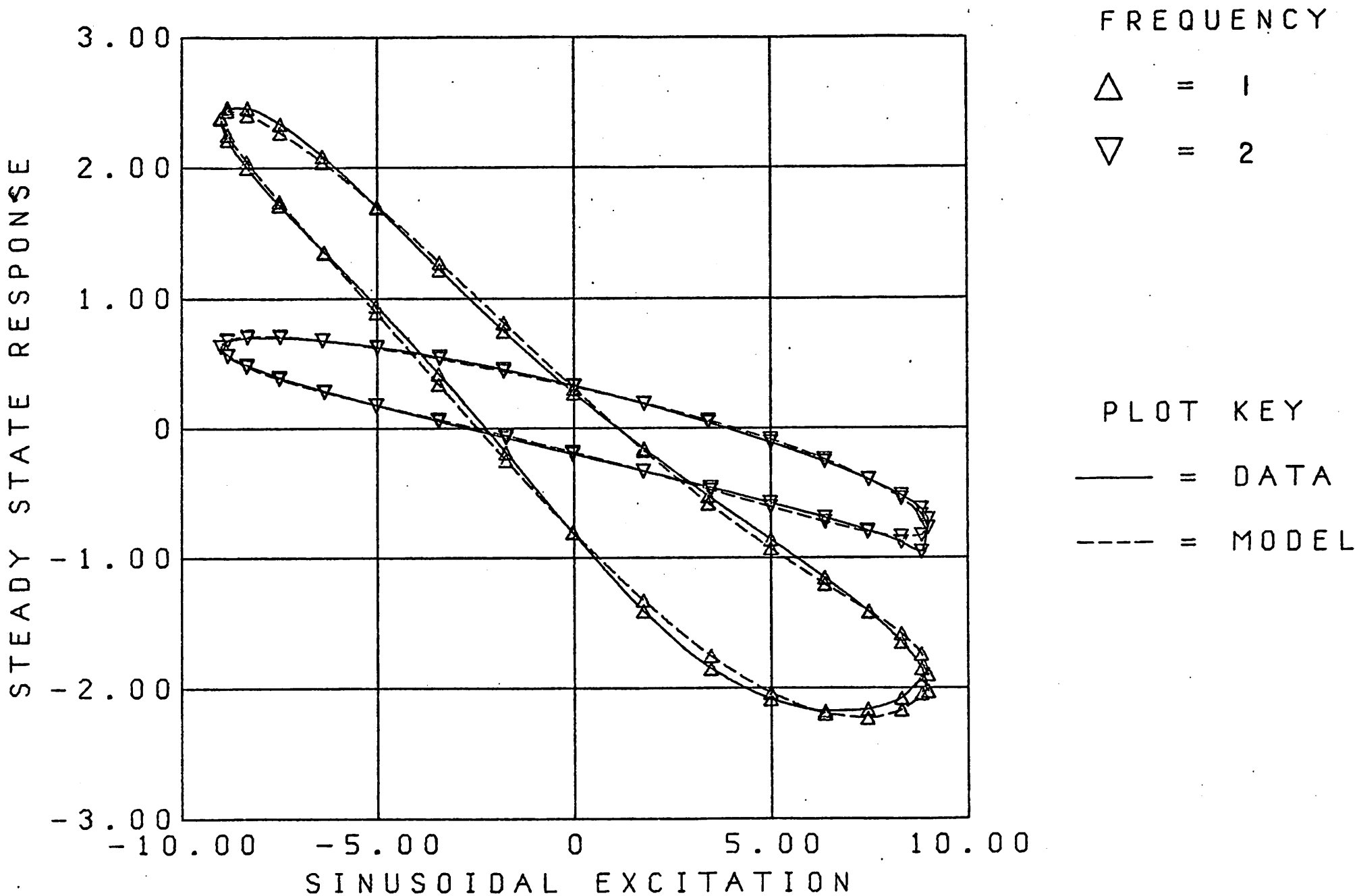


Fig. 3b. Steady State Response of System and Model for the Forced Van der Pol Equation with  $N = 3$ .

FREQUENCY

$\triangle$  = 1

$\nabla$  = 2

PLOT KEY

— = DATA

--- = MODEL

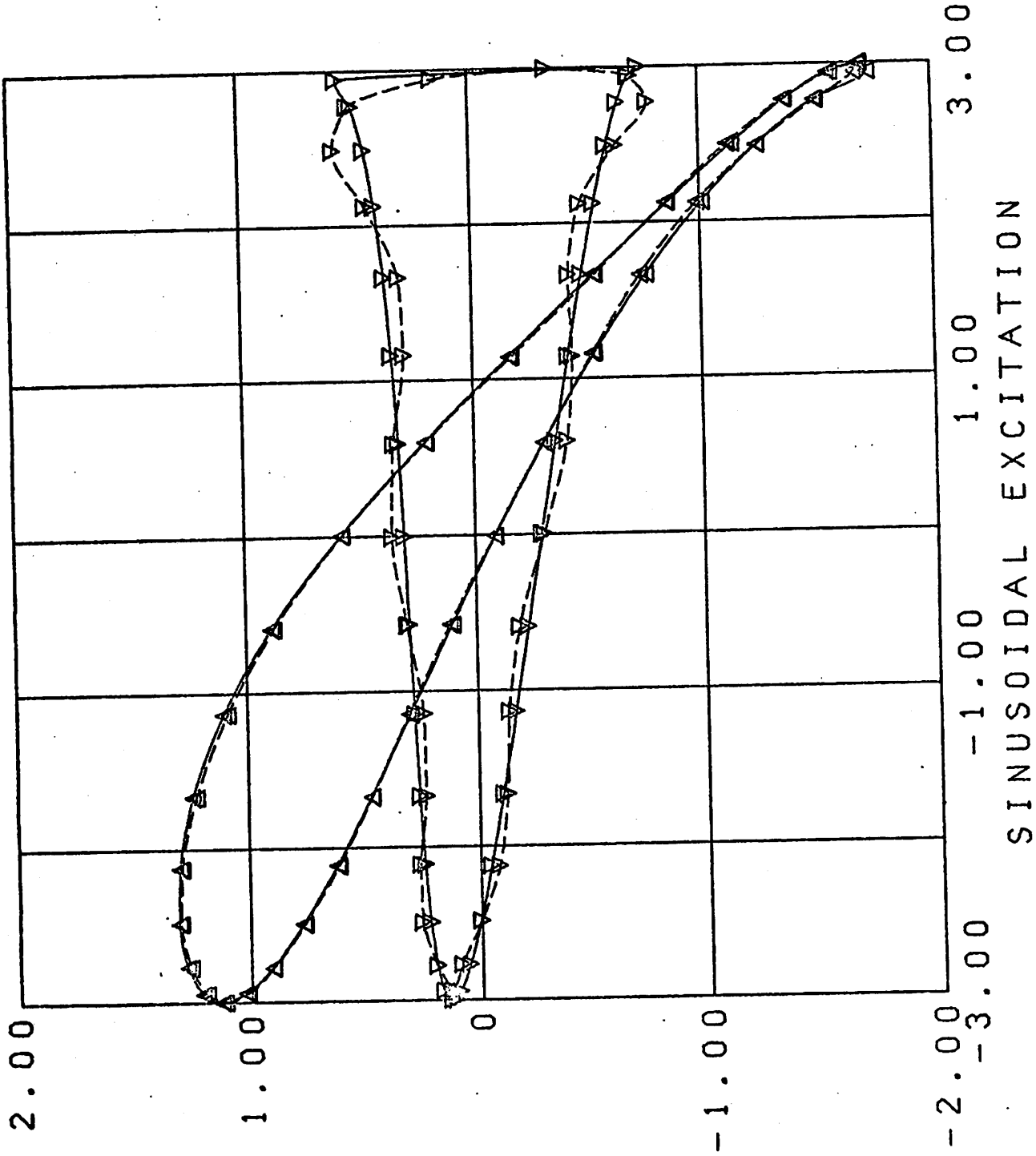


Fig. 4a. Steady State Response of System and Model for the Forced Van der Pol Equation with  $N = 6$ .

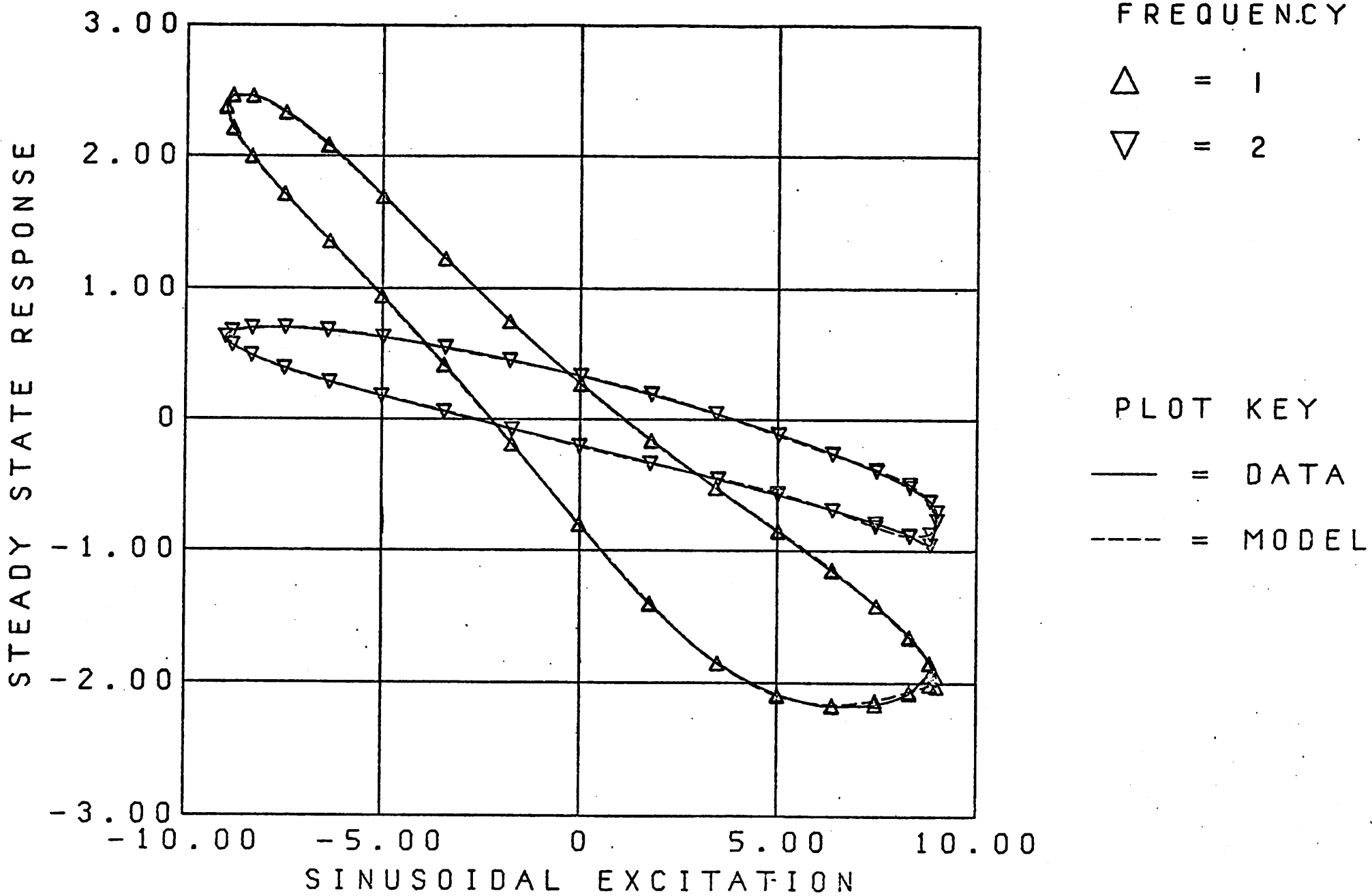


Fig. 4b. Steady State Response of System and Model for the Forced Van der Pol Equation with  $N = b$ .

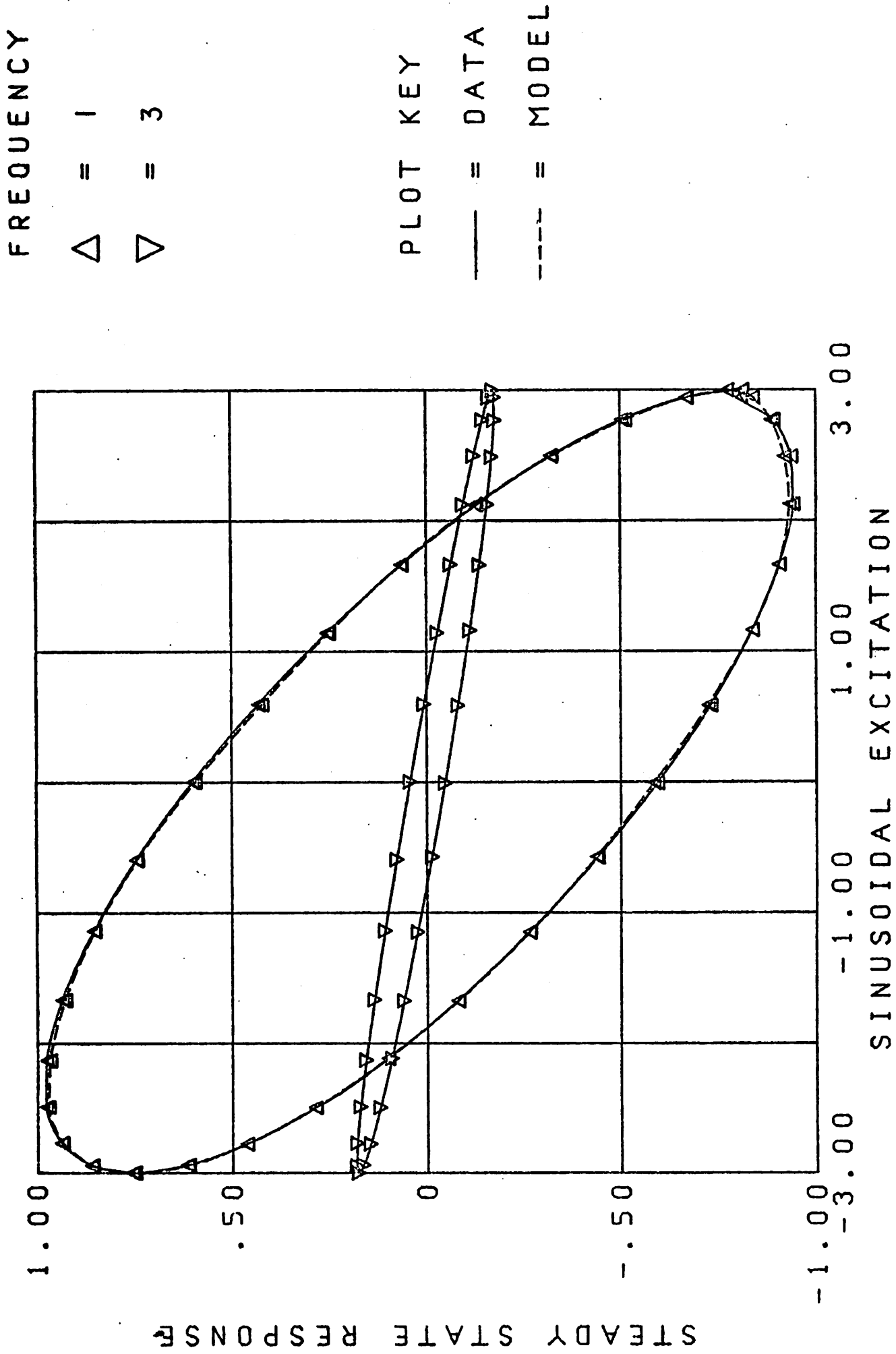


Fig. 5a. Steady State Response of System and Model for the Forced Duffing Equation with  $N = 6$ .

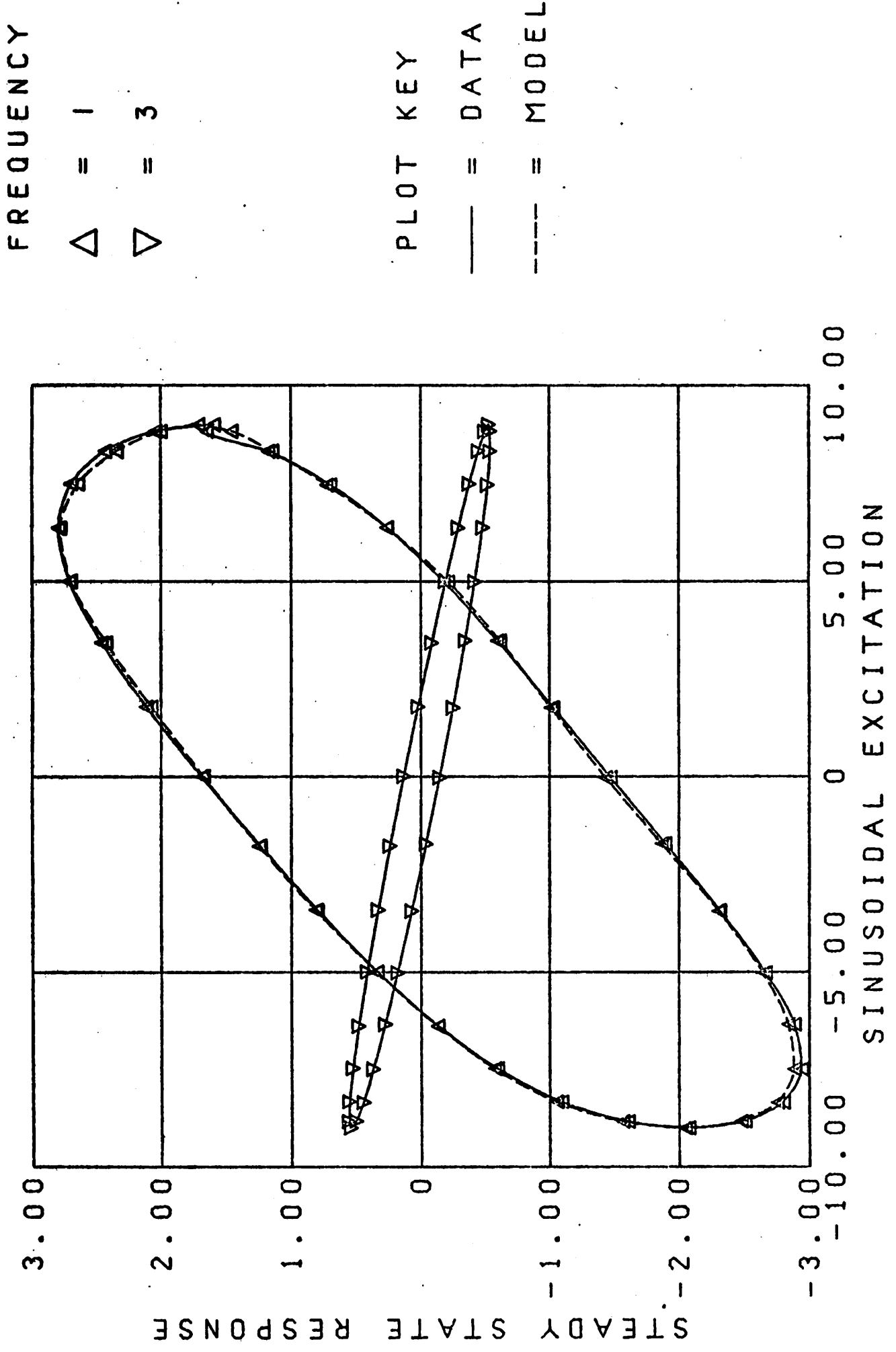


Fig. 5b. Steady State Response of System and Model for the Forced Duffing Equation with  $N = 6$ .

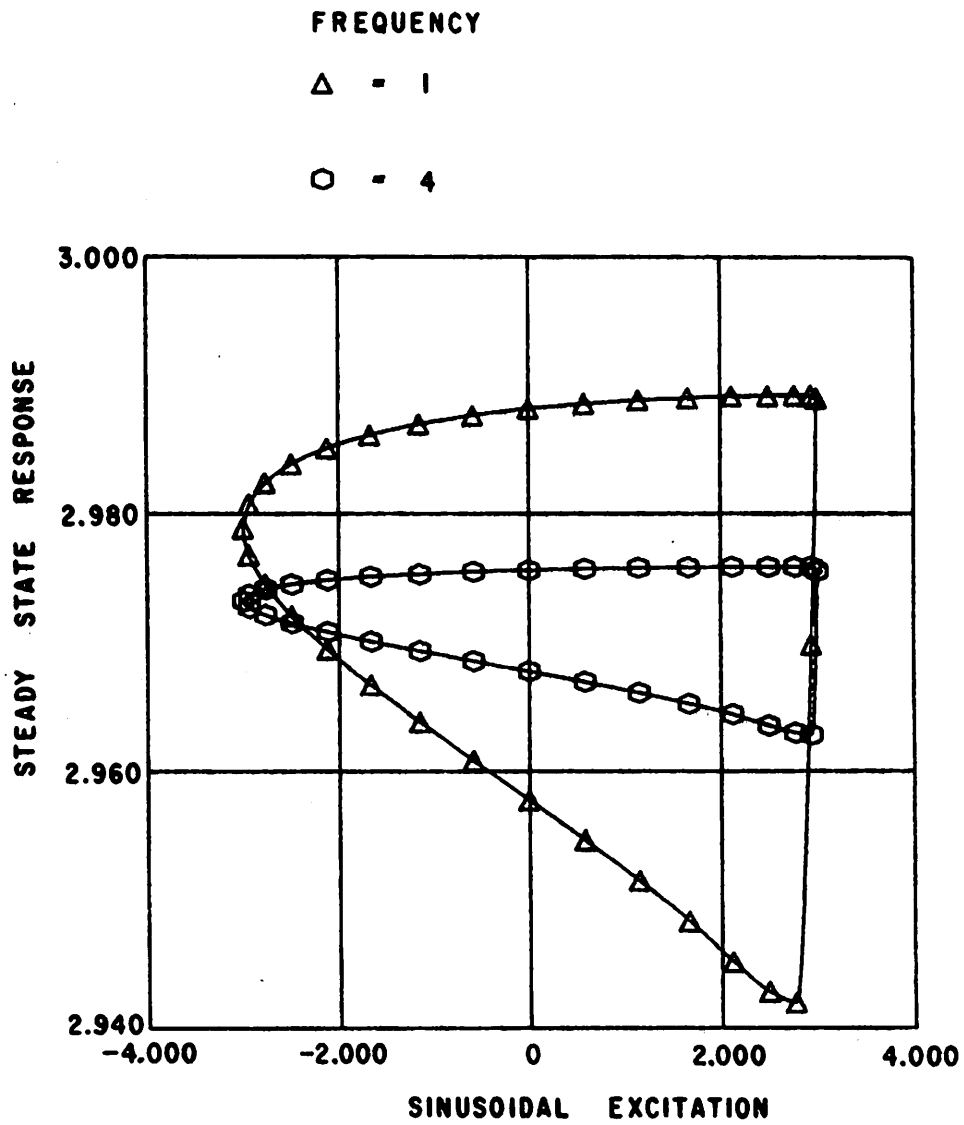


Fig. 6a. Steady State Response of Amplitude Detection Subsystem Under Sinusoidal Excitation.

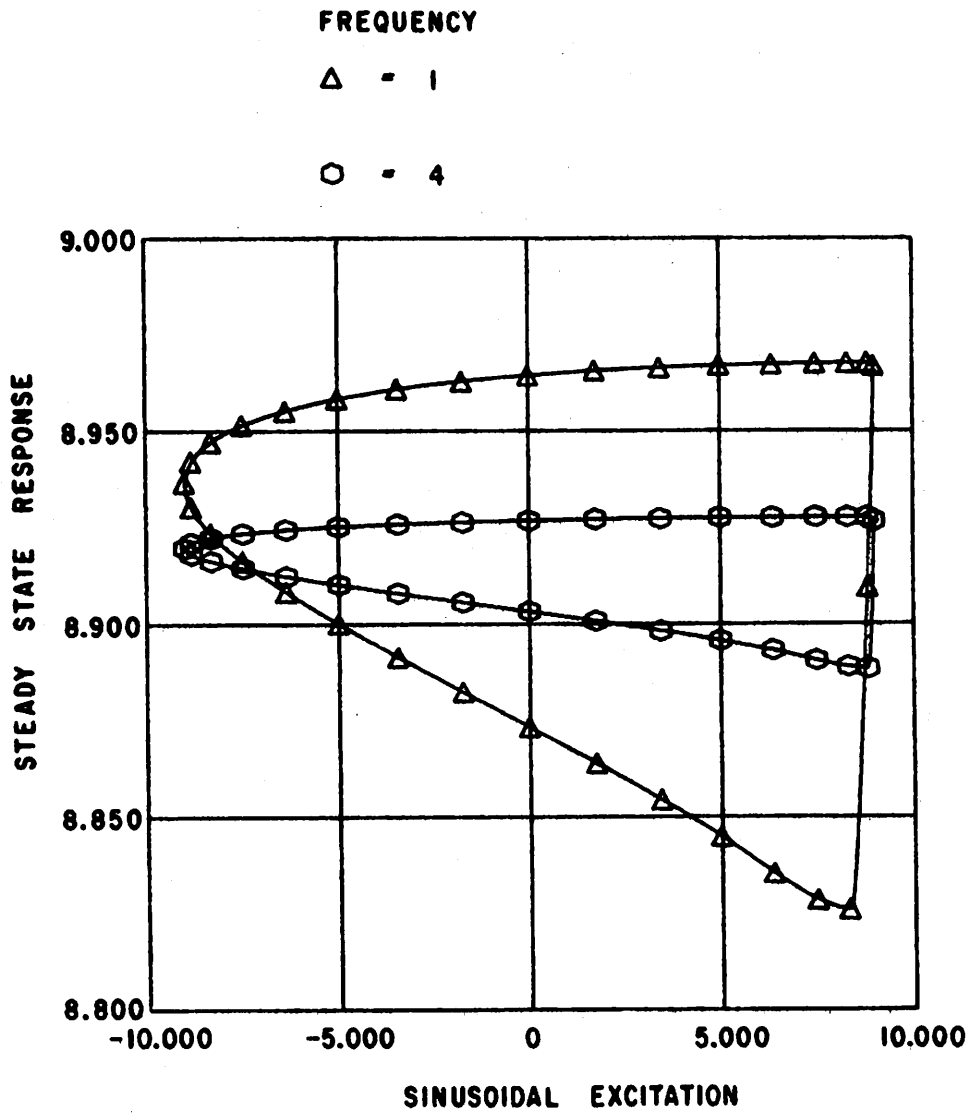


Fig. 6b. Steady State Response of Amplitude Detection Subsystem Under Sinusoidal Excitation.